**Tenth International Congress
on Sound and Vibration**
7-10 July 2003 • Stockholm, Sweden

NUMERICAL MODELLING OF RUBBER VIBRATION ISOLATORS

Clemens A.J. Beijers and André de Boer

University of Twente
P.O. Box 217, 7500 AE Enschede, The Netherlands
email: c.a.j.beijers@utwente.nl

Abstract

An important cause for interior noise in vehicles is structure-borne sound from the engine. The vibrations of the source (engine) are transmitted to the receiver structure (the vehicle) causing interior noise in the vehicle. For this reason the engine is supported by rubber isolators for passive isolation in especially the high-frequency region. To make a good judgment of the characteristics of a vibration isolator in the design process, it is useful to use numerical models.

In this paper a cylindrical vibration isolator is modelled numerically with the Finite Element package ABAQUS. The investigation is split in two parts: first a nonlinear analysis is performed for different pre-deformations of the mount. After that, a linear harmonic analysis is superimposed on the pre-deformed isolator. The structure-borne sound is transmitted by the isolator by six degrees of freedom, so the harmonic analysis must be performed for different excitations. With the results the behavior of the isolator can be represented by dynamic stiffness matrices as function of the frequency and pre-deformation. These matrices can be used to model the passive isolation components as part of numerical models of hybrid isolation systems. These isolation systems describe a combination of active and passive isolation to reduce the structure-borne sound transmission to receiver structures.

805

INTRODUCTION

The isolation behavior of rubber isolators strongly depends on the excitation frequency and the pre-deformation of the mount as consequence of the weight of the source to be isolated. A lot of research has been done on this topic, both experimentally [4],[7],[2] and in the field of modelling [5],[1]. In general the behavior of isolators are characterized by a dynamic impedance or dynamic stiffness matrix, measured or simulated as function of the frequency and pre-deformation. In this paper the dynamic stiffness matrix formulation will be used to characterize the behavior of the rubber isolator or mount. Generally, the described models in the literature focus on the behavior of isolators in the longitudinal direction, because in the static case this direction has the most dominant stiffness. For transmission of structure-borne sound (the transmitted power through the mounts that result in radiated sound at the receiver structure) the transfer of each of the six degrees of freedom may play an important role. To take account of the pre-deformation and to determine the total dynamic stiffness matrices in six degrees of freedom, a numerical model is made of an cylindrical isolator. For this purpose the finite element package ABAQUS is used. The dynamic stiffness matrices will be determined for an isolator described in the literature and for which all material parameters have been determined that are necessary to do the simulations [3]. A lot of experiments have been performed on the described isolator, so the numerical results can be validated with the experimental results [4]. The dynamic transfer matrices provide information on and insight in the isolation behavior of the mount and can also be used to couple with transfer matrices of receivers and sources to examine the coupled behavior.

PROCEDURE

The behavior of the mount is described by a field representation at the junction at the top ① (connection with the source) and the bottom ② (connection with the receiver) of the mount as depicted in figure 1. At the junctions the forces and displacements deform the mount in six degrees of freedom. A convenient relation between the forces and displacements can be defined by means of a two-port network [6] in terms of the blocked dynamic driving point stiffness matrices $\mathbf{k}_{11}$ and $\mathbf{k}_{22}$ and blocked dynamic transfer stiffness matrices $\mathbf{k}_{12}$ and $\mathbf{k}_{21}$ according to:

$$\mathbf{f}|_1 = \mathbf{k}_{11}\mathbf{u}|_1 + \mathbf{k}_{12}\mathbf{u}|_2 \tag{1}$$

$$\mathbf{f}|_2 = \mathbf{k}_{21}\mathbf{u}|_1 + \mathbf{k}_{22}\mathbf{u}|_2 \tag{2}$$

where $|_1 \, |_2$ means acting at top (port number one) and bottom (port number two), respectively. This type of representation is only valid for linear systems and it is assumed that the force and displacement vectors and stiffness matrices depend on frequency. For the considered application it is necessary that the steel plates (at the top and bottom of the mount) behave as rigid moving plates. This is in general valid for rubber isolators, because the vulcanized rubber is firmly bonded with two metal plates at the top and bottom. Each dynamic stiffness matrix contains 36 (6x6) components, but the number
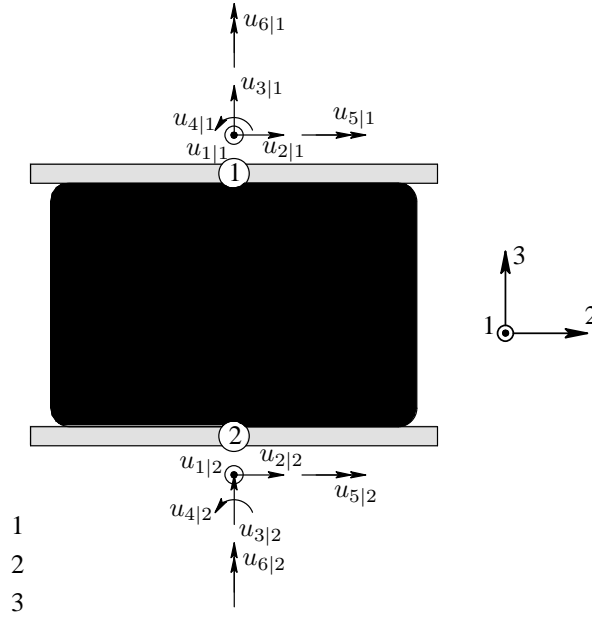
Figure 1: Vibration isolator with field representation at top ① and bottom ② with the displacement vector in positive directions. The same convention is applied for the force components.

of independent dynamic stiffness components can be reduced considerably depending on the geometry of the mount. The analysis is split in two parts: first a pre-deformation is applied to take account of the static deformation due to the weight of the source. In general large deformations are involved due to the large pre-deformation and a nonlinear analysis is necessary. After that a linear harmonic analysis is superimposed on the pre-deformed isolator, hereby assuming that the vibration amplitudes are sufficiently small to justify a linearized model.

For the cylindrical mount it can be derived with help of reciprocity that $\mathbf{k}_{12}$ is equal to $\mathbf{k}_{21}^T$. Also the driving point stiffness matrix $\mathbf{k}_{22}$ has the same components as the stiffness matrix $\mathbf{k}_{11}$, except differences in plus and minus signs. The number of components of the dynamic stiffness matrices (36 for each matrix) to be determined can be reduced considerably for a cylindrical isolator (see [7], also for an overview of other types of isolators). For the blocked driving point and transfer stiffness $\mathbf{k}_{11}$ and $\mathbf{k}_{21}$ the following non-zero components have to be determined:

$$
\begin{aligned}
k_{11}(1,1) &= k_{11}(2,2) & k_{21}(1,1) &= k_{21}(2,2) \\
k_{11}(3,3) & & k_{21}(3,3) & \\
k_{11}(4,4) &= k_{11}(5,5) & k_{21}(4,4) &= k_{21}(5,5) \\
k_{11}(6,6) & & k_{21}(6,6) & \\
k_{11}(2,4) = k_{11}(4,2) &= & k_{21}(2,4) = -k_{21}(4,2) &= \\
-k_{11}(1,5) &= -k_{11}(5,1) & -k_{21}(1,5) &= k_{21}(5,1)
\end{aligned}
\tag{3}
$$

with all other components equal to zero. To determine the components, in fact only four different types of simulations have to be made as depicted in figure 2. For each
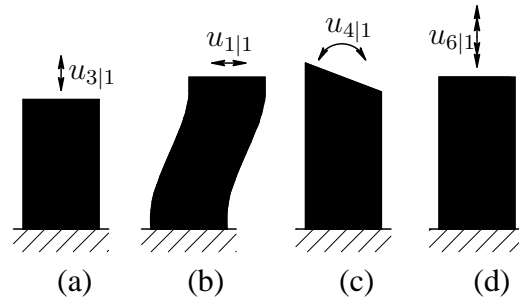
807

1
2

Figure 2: Performed simulations for the cylindrical vibration isolator with its quasi-statical deformed shape.

simulation the bottom plate is clamped and the harmonic displacement amplitude of one degree of freedom of the top plate is prescribed, while maintaining the other degrees of freedom equal to zero. The pre-deformation has already been determined. After that the reaction forces can be determined at the nodes on the top and the bottom of the mount. These nodal forces can be transformed to one equivalent force vector acting at the junctions of the mount. The procedure can be summarized as:

- non-linear calculation of pre-deformation

- harmonic analysis superposed on the pre-deformed geometry and material with prescribed displacement amplitude at top of the mount

- calculation of equivalent nodal forces and moments at the center of the top plate (for components of $\mathbf{k}_{11}$) and bottom plate (for components of $\mathbf{k}_{21}$).

- composition of the dynamic transfer and driving point stiffness matrices

NUMERICAL MODEL

The simulated cylindrical isolator and material behavior of the rubber material is extensively described in the literature [3]. The parameters are chosen equal to the isolator tested in this thesis and are depicted in figure 3. The material model used for the simulations is the Yeoh model, requiring three parameters.

In figure 3(b) the three-dimensional mesh of the isolator is shown. The rubber material is meshed with linear solid elements (type C3D8H) and the steel plates at the top and bottom are represented by linear shell elements (type S4R).

RESULTS

Following the described procedure the different components of the dynamic stiffness matrix as given in equation (3) can be determined. In figure 5 the different dynamic transfer stiffness components are depicted. The driving point transfer matrices can be determined and depicted in the same way, but are not displayed here.

Parameter	Value
density	1050 kg/m^3
Yeoh model:	
C_{10}	$\mu_\infty/2 = 2.97 \cdot 10^5 \text{ N/m}^2$
C_{20}	$-4.5 \cdot 10^4 \text{ N/m}^2$
C_{30}	$1.5 \cdot 10^4 \text{ N/m}^2$
D_1	$2/k_0 = 1.515 \cdot 10^{-9} \text{ N/m}^2$
Shear mod. :	
μ_∞	$5.94 \cdot 10^5 \text{ N/m}^2$
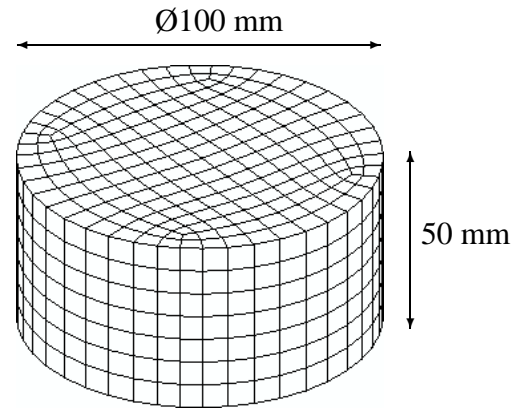
(b) Three-dimensional mesh

Figure 3: Properties and dimensions of simulated isolator.

The influence of the pre-deformation is considerable for the longitudinal dynamic stiffness, see figure 5(b). Besides the change in geometry, the pre-deformation also influences the material behavior due to stiffening. It can be seen that the magnitude of the dynamic longitudinal stiffness increases as function of the pre-deformation at low frequencies: this is mainly due to the increase of the cross-sectional area of the isolator. The influence of the pre-deformation on the other components of the dynamic transfer stiffness is much smaller.

The influence of the dynamic behavior is much larger than the influence of the pre-deformation. Considering the different transfer functions it can be concluded that in the first region the dynamic stiffness remains almost constant and nearly equal to the static stiffness. When the frequency of the excitation increases, the influence of the mass behavior of the mount also increases. When the excitation frequency is near the first anti-resonance frequency, the dynamic stiffness increases. At resonance frequencies the dynamic stiffness is in general minimal. The influences of the separate (anti)-resonances are difficult to distinguish from each other, due to the high damping of the rubber. The high damping is recognized by the wide amplitude peaks and smooth phase transitions of the transfer, and consequently a large modal overlap is involved. It can be seen that especially $k_{12}(1, 1)$ is very susceptible for the dynamic influences. It is remarkable that in the frequency range between 200 and 300 Hz the transversal dynamic stiffness exceeds the longitudinal dynamic stiffness. This means that in this frequency range the transmission of structure-borne sound can be dominated by the transverse excitation of the source. The simulated results of the dynamic stiffness matrices agreed in general quite well with the experimental results of the cylindrical vibration isolator as described in [4]. However, the dynamic transfer components $k_{12}(4, 4)$ and $k_{12}(2, 4)$ show some deviations in the height of the peaks.

As explained, for a cylindrical mount only four harmonic simulations are needed (for each pre-deformation) to describe its total isolation behavior. One component of the dynamic stiffness matrices is in fact determined twice: $k_{11}(2, 4) = -k_{11}(5, 1)$ and $k_{21}(2, 4) = k_{21}(5, 1)$. A convenient check of the simulations can be made by comparing

these transfers with each other. For the described simulations these results matched very well.

To give an idea of the deformation of the mount, the longitudinal dynamic transfer stiffness is considered in more detail. The longitudinal transfer is the only transfer that can be analyzed with an axial-symmetric analysis. The harmonically deformed shape is plotted in figure 4 for the axial-symmetric model of a mount without pre-deformation. The pictures are contour plots of the real part of the longitudinal displacement (along the axis) and the imaginary part. The displacement at the top-side is prescribed, the bottom-side is clamped. It can be seen that up to a frequency of about 350 Hz the harmonically deformed shape resembles the static shape. After that a wave is introduced, first leading to an anti-resonance (450 Hz) recognized by the increase in the dynamic stiffness. After the anti-resonance the influence of a resonance arises, indicated by the decrease of the dynamic stiffness. When the outer-boundary of the rubber material is studied it can be seen that the wavelength decreases with increasing frequency of the excitation. Also waves are formed internally in the rubber, resulting in a sort of dynamic shearing motion. It must be noted that due to the non-proportional damping the standing waves are not synchronous, meaning that the nodal lines travel through the rubber during a period (indicated by the complex displacement field in figure 4).
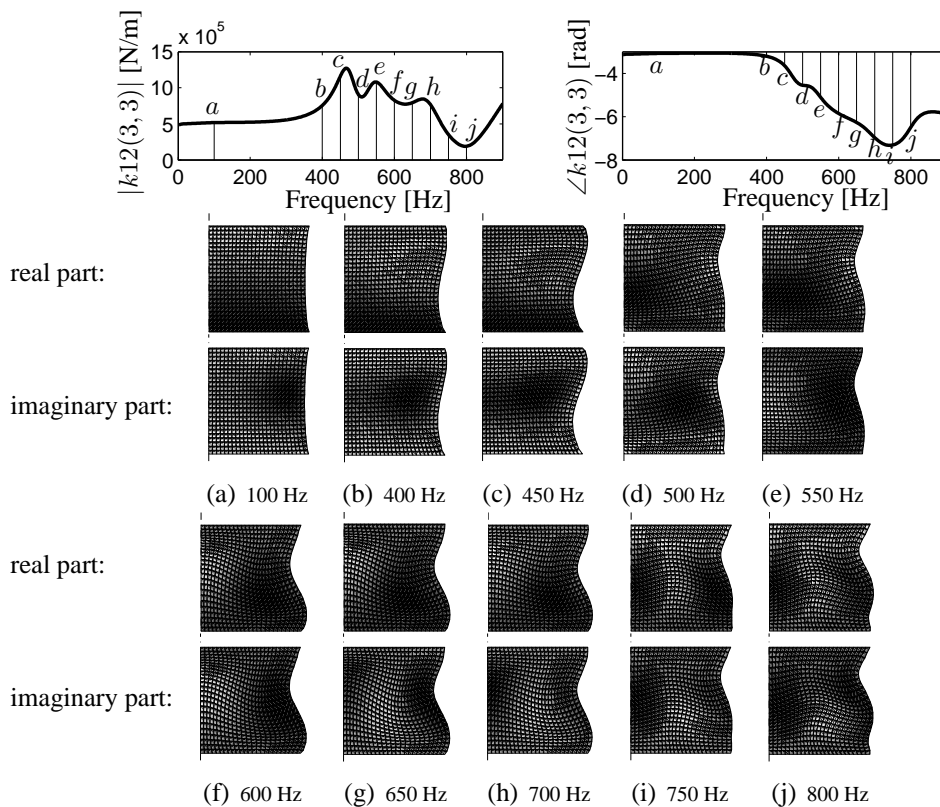

Figure 4: Contour plots of the longitudinal displacement on the deformed shape of an axial-symmetric part of the isolator.
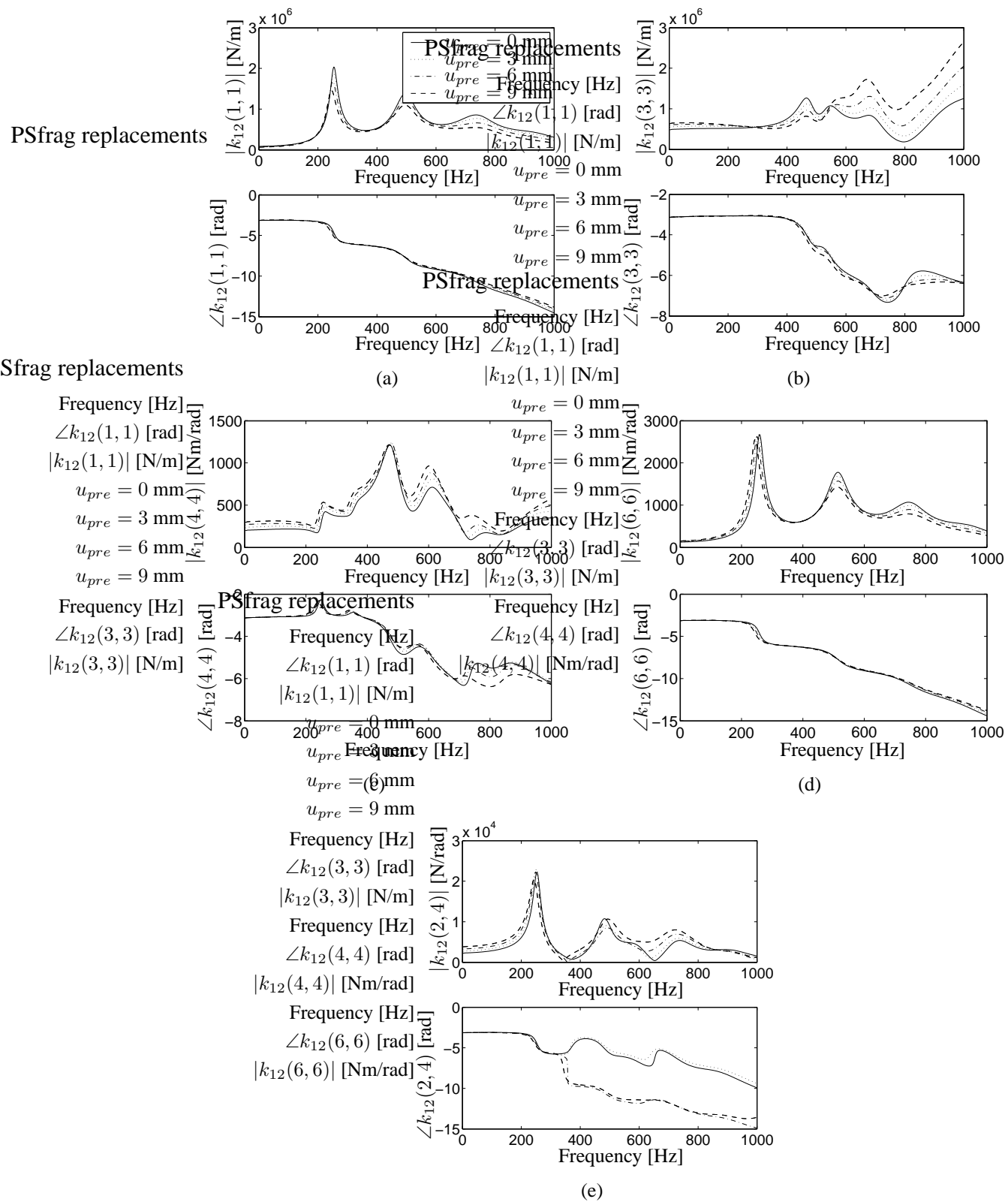
Figure 5: Components of the transfer point stiffness matrix for different pre-loads.

CONCLUSION

The behavior of rubber mounts in terms of the dynamic driving point stiffness matrix and dynamic transfer stiffness matrix, can be determined rather accurately with ABAQUS. The influence of the pre-deformation and the dynamic behavior was predicted quite well. However, the dynamic transfer components $k_{12}(4,4)$ and $k_{12}(2,4)$ showed some deviations in the height of the peaks in comparison with the experimental results.

The influence of the dynamic behavior on the dynamic stiffness behavior is considerable on all components of the dynamic transfer stiffness. The pre-deformation has only a large influence on the longitudinal transfer stiffness. The harmonic deformation of the rubber is quite complex due to the material behavior of the rubber: rubber behaves nearly incompressible and has a lot damping. The dynamic stiffness matrices can be used as part of more extensive models, e.g. coupling with receiver and source models to predict the behavior of isolation systems.

ACKNOWLEDGEMENTS

REFERENCES

[1] J.D. Dickens. Dynamic model of vibration isolator under static load. *Journal of Sound and Vibration*, 236(2):323–337, 2000.

[2] J.D. Dickens and C.J. Norwood. Universal method to measure dynamic performance of vibration isolators under static load. *Journal of Sound and Vibration*, 244(4):685–696, 2001.

[3] L. Kari. *Structure-borne sound properties of vibration isolators*. PhD dissertation, KTH - Royal Institute of Technology, Stockholm, 1998.

[4] L. Kari. Dynamic transfer stiffness measurements of vibration isolators in the audible frequency range. *Noise Control Engineering Journal*, 49(2):88–102, 2001.

[5] L. Kari. On the waveguide modelling of dynamic stiffness of cylindrical vibration isolators. part I: the model, solution and experimental comparison. *Journal of Sound and Vibration*, 244(2):211–233, 2001.

[6] J.C. Snowdon. Universal method to measure dynamic performance of vibration isolators under static load. *Journal of the Acoustical Society of America*, 66(5):1245–1274, 1979.

[7] J.W. Verheij. *Multi-path sound transfer from resiliently mounted shipboard machinery*. PhD dissertation, Institute of Applied Physics TNO-TH, Delft, 1986.